UC Berkeley
Archaeological X-ray Fluorescence Reports

Title
SOURCE PROVENANCE OF OBSIDIAN ARTIFACTS FROM 48PA3604, PARK COUNTY, WYOMING

Permalink
https://escholarship.org/uc/item/2363q9qj

Author
Shackley, M. Steven

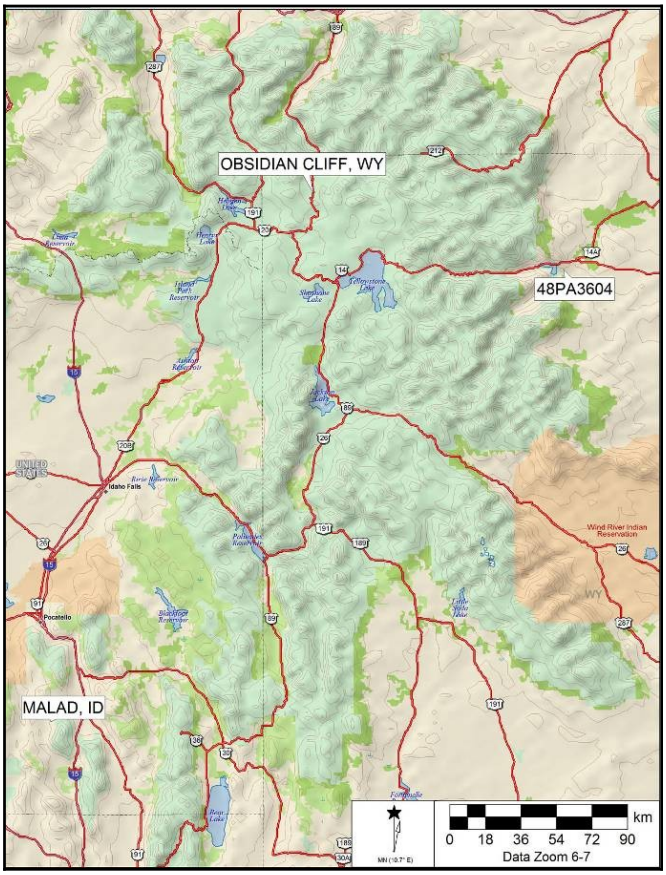
Publication Date
2020-05-20

eScholarship.org Powered by the California Digital Library
University of California

GEOARCHAEOLOGICAL XRF LAB
A GREEN SOLAR FACILITY

GEOARCHAEOLOGICAL X-RAY FLUORESCENCE SPECTROMETRY LABORATORY
8100 Wyoming Blvd., Ste M4-158 Albuquerque, NM 87113
USA

SOURCE PROVENANCE OF OBSIDIAN ARTIFACTS FROM 48PA3604, PARK COUNTY, WYOMING



General location of the project site and the two sources of archaeological obsidian in the assemblage

by

M. Steven Shackley, Ph.D., Director
Geoarchaeological XRF Laboratory
Albuquerque, New Mexico

Report Prepared for

Professor Laura Scheiber
Department of Anthropology
Indiana University, Bloomington

20 May 2020

INTRODUCTION

The analysis here of 19 obsidian artifacts from 48PA3604 in Wyoming is dominated by Obsidian Cliff, Yellowstone Volcanic Field obsidian as in previous projects in the region, with two artifacts produced from the Malad, Idaho source (see cover image and Table 1 and Figure 1). One artifact is produced from an, as yet, unlocated source that was not in the Skinner/Shackley North American obsidian source database.

LABORATORY SAMPLING, ANALYSIS AND INSTRUMENTATION

All archaeological samples were analyzed whole. The results presented here are quantitative in that they are derived from "filtered" intensity values ratioed to the appropriate x-ray continuum regions through a least squares fitting formula rather than plotting the proportions of the net intensities in a ternary system (McCarthy and Schamber 1981; Schamber 1977). Or more essentially, these data through the analysis of international rock standards, allow for inter-instrument comparison with a predictable degree of certainty (Hampel 1984; Shackley 2011).

All analyses for this study were conducted on a ThermoScientific *Quant'X* EDXRF spectrometer, located at the Geoarchaeological XRF Laboratory, Albuquerque, New Mexico. It is equipped with a thermoelectrically Peltier cooled solid-state Si(Li) X-ray detector, with a 50 kV, 50 W, ultra-high-flux end window bremsstrahlung, Rh target X-ray tube and a 76 μm (3 mil) beryllium (Be) window (air cooled), that runs on a power supply operating from 4-50 kV/0.02-1.0 mA at 0.02 increments. The spectrometer is equipped with a 200 l min^{-1} Edwards vacuum pump, allowing for the analysis of lower-atomic-weight elements between sodium (Na) and titanium (Ti). Data acquisition is accomplished with a pulse processor and an analogue-to-digital converter. Elemental composition is identified with digital filter background removal, least squares empirical peak deconvolution, gross peak intensities and net peak intensities above background.

Trace Element Analysis

The analysis for mid Zb condition elements Ti-Nb, Pb, Th, the x-ray tube is operated at 30 kV, using a 0.05 mm (medium) Pd primary beam filter in an air path at 100 seconds livetime

to generate x-ray intensity $K\alpha_1$-line data for elements titanium (Ti), manganese (Mn), iron (as $Fe_2O_3^T$), cobalt (Co), nickel (Ni), copper, (Cu), zinc, (Zn), gallium (Ga), rubidium (Rb), strontium (Sr), yttrium (Y), zirconium (Zr), niobium (Nb), lead (Pb), and thorium (Th). Not all these elements are reported since their values in many volcanic rocks are very low and below detection limits. Trace element intensities were converted to concentration estimates by employing a linear calibration line ratioed to the Compton scatter established for each element from the analysis of international rock standards certified by the National Institute of Standards and Technology (NIST), the US. Geological Survey (USGS), Canadian Centre for Mineral and Energy Technology, and the Centre de Recherches Pétrographiques et Géochimiques in France (Govindaraju 1994). Line fitting is linear (XML) for all elements. When barium (Ba), lanthanum (La), and cerium (Ce) are analyzed in the High Zb condition, the Rh tube is operated at 50 kV and up to 1.0 mA, ratioed to the bremsstrahlung region (see Davis 2011; Shackley 2011). Further details concerning the petrological choice of these elements in North American obsidians is available in Shackley (1988, 1995, 2005; Shackley et al. 2016, 2018, 2019; also Mahood and Stimac 1991; and Hughes and Smith 1993). Nineteen specific pressed powder standards are used for the best fit regression calibration for elements Ti-Nb, Pb, Th, Ba, La, and Ce include G-2 (basalt), AGV-2 (andesite), GSP-2 (granodiorite), SY-2 (syenite), BHVO-2 (hawaiite), STM-1 (syenite), QLO-1 (quartz latite), RGM-1 (obsidian), W-2 (diabase), BIR-1 (basalt), SDC-1 (mica schist), TLM-1 (tonalite), SCO-1 (shale), NOD-A-1 and NOD-P-1 (manganese) all US Geological Survey standards, NIST-278 (obsidian), U.S. National Institute of Standards and Technology, BE-N (basalt) from the Centre de Recherches Pétrographiques et Géochimiques in France, and JR-1 and JR-2 (obsidian) from the Geological Survey of Japan (Govindaraju 1994).

Statistical and Graphical Source Assignment.

The data from the WinTrace™ software were translated directly into Excel for Windows software for manipulation and on into JMP 12.0.1 for statistical analyses. In order to evaluate these quantitative determinations, machine data were compared to measurements of known

standards during each run. RGM-1 a USGS rhyolite standard is analyzed during each sample run of ≤ 19 for obsidian artifacts to check machine calibration (Table 1).

Source assignments were made by reference to the laboratory Skinner/Shackley data base and Davis et al. (1995). Further information on the laboratory instrumentation and source data can be found at: http://www.swxrflab.net. Trace element data exhibited in Table 1 and Figure 1 are reported in parts per million (ppm), a quantitative measure by weight.

REFERENCES CITED

Davis, L.B., S.A. Aaberg, J.G. Schmitt, and A. M. Johnson, 1995, *The Obsidian Cliff Plateau Prehistoric Lithic Source, Yellowstone National Park, Wyoming*. National Park Service, Division of Cultural Resources Selection Series 6, Denver, Colorado.

Davis, M.K., T.L. Jackson, M.S. Shackley, T. Teague, and J. Hampel, 2011, factors affecting the energy-dispersive x-ray fluorescence (EDXRF) analysis of archaeological obsidian. In *X-Ray Fluorescence Spectrometry (XRF) in Geoarchaeology*, edited by M.S. Shackley, pp. 45-64. Springer, New York.

Govindaraju, K., 1994 , 1994 compilation of working values and sample description for 383 Geostandards. *Geostandards Newsletter* 18 (special issue).

Hampel, Joachim H., 1984, Technical considerations in x-ray fluorescence analysis of obsidian. In *Obsidian Studies in the Great Basin*, edited by R.E. Hughes, pp. 21-25. Contributions of the University of California Archaeological Research Facility 45. Berkeley.

Hildreth, W., 1981, Gradients in silicic magma chambers: implications for lithospheric magmatism. *Journal of Geophysical Research* 86:10153-10192.

Hughes, Richard E., and Robert L. Smith, 1993, Archaeology, geology, and geochemistry in obsidian provenance studies. *In Scale on Archaeological and Geoscientific Perspectives*, edited by J.K. Stein and A.R. Linse, pp. 79-91. Geological Society of America Special Paper 283.

Mahood, Gail A., and James A. Stimac, 1990, Trace-element partitioning in pantellerites and trachytes. *Geochemica et Cosmochimica Acta* 54:2257-2276.

McCarthy, J.J., and F.H. Schamber, 1981, Least-squares fit with digital filter: a status report. In *Energy Dispersive X-ray Spectrometry*, edited by K.F.J. Heinrich, D.E. Newbury, R.L. Myklebust, and C.E. Fiori, pp. 273-296. National Bureau of Standards Special Publication 604, Washington, D.C.

Schamber, F.H., 1977, A modification of the linear least-squares fitting method which provides continuum suppression. In *X-ray Fluorescence Analysis of Environmental Samples*, edited by T.G. Dzubay, pp. 241-257. Ann Arbor Science Publishers.

Shackley, M.S., 1988, Sources of Archaeological Obsidian in the Southwest: An Archaeological, Petrological, and Geochemical Study. *American Antiquity* 53:752-772.

Shackley, M. S.,1995, Sources of archaeological obsidian in the greater American Southwest: an update and quantitative analysis. *American Antiquity* 60(3):531-551.

Shackley, M.S., 2005, *Obsidian: Geology and Archaeology in the North American Southwest*. University of Arizona Press, Tucson.

Shackley, M.S., 2011, An introduction to x-ray fluorescence (XRF) analysis in archaeology. In *X-Ray Fluorescence Spectrometry (XRF) in Geoarchaeology*, M.S. Shackley (Ed.), pp. 7-44. Springer, New York.

Shackley, M.S., L.E. Morgan, and D. Pyle, 2018, Elemental, isotopic, and geochronological variability in Mogollon-Datil Volcanic Province archaeological obsidian, southwestern USA: solving issues of inter-source discrimination. *Geoarchaeology* 33:486-497.

Shackley, M.S., 2019, Natural and cultural history of the Obsidian Butte source, Imperial County, California. *California Archaeology* 11: 21-44.

Shackley, M.S., F. Goff, and S.G. Dolan, 2016, Geologic origin of the source of Bearhead rhyolite (Paliza Canyon) obsidian, Jemez Mountains, Northern New Mexico. *New Mexico Geology* 38:52-62.

Table 1. Elemental concentrations for the archaeological samples and USGS RGM-1 rhyolite standard. All measurement in parts per million (ppm).

Sample	Ti	Mn	Fe	Rb	Sr	Y	Zr	Nb	Ba	Ce	Pb	Th	Source
1	1258	266	10145	131	80	34	99	10	1765	31	32	21	Malad, ID
3	937	262	10603	234	10	79	205	46	93	140	30	35	unknown
4	892	249	11313	237	12	72	163	40	60	63	32	28	Obsidian Cliff, WY
5	959	264	11282	248	14	69	167	51	34	47	27	34	Obsidian Cliff, WY
6	999	276	12291	269	10	79	177	45	26	70	39	30	Obsidian Cliff, WY
7	1094	239	11004	242	9	73	163	43	0	48	32	25	Obsidian Cliff, WY
8	806	262	11082	243	9	75	165	42	51	53	29	23	Obsidian Cliff, WY
9	891	253	11220	259	10	77	174	47	76	64	32	27	Obsidian Cliff, WY
10	1195	247	10849	218	12	64	142	40	11	40	30	31	Obsidian Cliff, WY
11	917	254	11528	262	12	75	171	45	52	71	32	37	Obsidian Cliff, WY
12	1056	237	10637	228	11	74	158	47	69	37	28	30	Obsidian Cliff, WY
13	927	268	11762	257	12	78	166	48	8	49	38	35	Obsidian Cliff, WY
14	1176	235	10938	225	16	69	154	38	0	34	30	30	Obsidian Cliff, WY
15	998	245	10692	226	13	69	161	41	61	67	30	35	Obsidian Cliff, WY
16	917	246	11287	251	13	75	170	49	84	57	32	28	Obsidian Cliff, WY
17	1244	272	9760	126	77	28	91	17	1774	58	26	14	Malad, ID
18	984	241	11438	259	9	74	176	47	36	55	34	36	Obsidian Cliff, WY
20	907	257	11219	244	9	70	171	42	50	88	32	35	Obsidian Cliff, WY
21	842	245	10980	244	13	75	169	44	46	117	33	25	Obsidian Cliff, WY
RGM1-	151	28	1319	14	10	2	22	6	795	38	1	6	standard

S4	3	6	5	6	8	8	5				7		

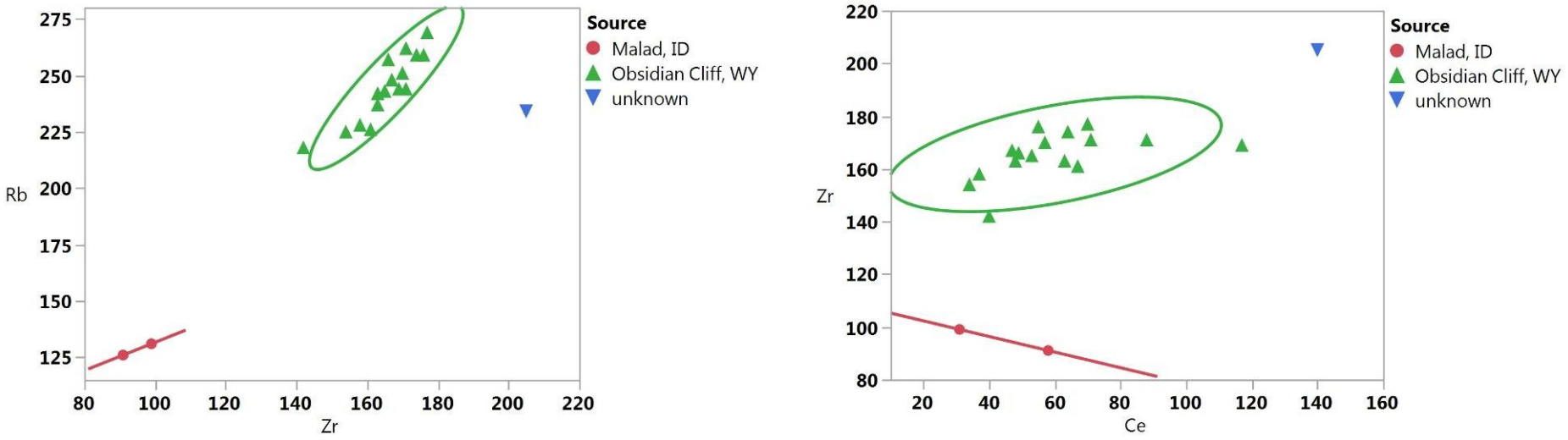


Figure 1. Zr/Rb and Ce/Zr bivariate plots of the archaeological samples. Confidence ellipses at 95%.